Thin Solid Films 519 (2011) 2366 – 2370

Sputtering of ZnO:Al films from dual tube targets with tilted magnetrons

H. Zhu[1, 2, *], E. Bunte[1], J. Hüpkes[1], S. M. Huang[2]

[1] IEF5-Photovoltaik, Forschungszentrum Jülich GmbH, D-52425 Jülich, Germany

[2]Engineering Research Center for Nanophotonics and Advanced Instrument, Ministry of Education, East China Normal University, 200062, Shanghai, P.R. China

Abstract

Aluminum doped zinc oxide (ZnO:Al) films were deposited by mid-frequency (MF) sputtering rotating tube targets at high discharge powers in a double cathode system. The magnetrons located inside the tube targets were tilted by ±30°, leading to different racetrack orientations. Deposition rate and electrical properties of statically deposited films were investigated. Different properties of ZnO:Al films show lateral variations corresponding to the racetrack positions, which shift according to the tilt angles of double magnetrons. The highest average static deposition rate and the corresponding dynamic value were up to 360 nm/min and 111 nm·m/min, respectively, for magnetrons tilted towards the center of the cathodes. The material properties of ZnO:Al film prepared in dynamic mode were found to behave like the superpositions of properties of static films at different positions. Upon wet chemical etching in diluted hydrochloric acid (HCl), the surfaces of sputtered ZnO:Al films became rough, and three typical surface structures were observed and identified on statically deposited ZnO:Al films. The related plasma physics, growth and chemical etching mechanisms were discussed.

Key words: ZnO:Al films, Magnetron sputtering, Wet etching

1. Introduction

Aluminum doped zinc oxide thin films (ZnO:Al) have been widely used as transparent conductive electrodes for optoelectronic devices, especially for thin-film solar cells due to their excellent optical and electrical properties [**1**]. Upon wet chemical etching in hydrochloric acid (HCl) ZnO: Al thin films develop rough surface structures, leading to effective light-trapping when they are applied as front contact in silicon thin film solar cells [**2, 3**]. Magnetron sputtering is a cost-effective technology for manufacturing ZnO:Al films on large areas in industrial production [**4**, **5, 6, 7**].

In previous studies, most researchers employed planar ceramic targets [**2, 8**] or metallic targets [**5, 9, 10, 11**] for ZnO:Al film preparations. Recently, magnetron sputtering from rotatable ceramic tube targets to manufacture large area ZnO:Al films

has been applied [**15, 16, 17**]. High quality ZnO:Al films with excellent optical and electrical properties were presented. The influences of various deposition parameters like working pressure, substrate temperature as well as discharge power and argon gas flow on ZnO:Al films were investigated. All these investigations were based on dynamic deposition mode in in-line sputtering systems. In fact, the optical and electrical properties of these ZnO:Al films are comprehensive effects of sputtering at different positions in plasma during depositions. Therefore we can get a deeper insight into the relationship between sputtering conditions and film properties by studying static sputtering.

In this study, we investigate ZnO:Al films sputtered with mid-frequency (MF) excitation from rotatable double magnetrons in static mode. We study the influence of the magnetron tilt angles on the ZnO:Al film properties. Three different cases were investigated. The deposition rate, electrical properties and etching behavior in HCl of ZnO:Al films in dependence on substrate position, were studied. These film properties were compared to films deposited dynamically at the same deposition conditions.

2. Experimental

ZnO:Al films were prepared on 30×30 cm² float glasses at high deposition rates in a vertical in-line sputtering system (VISS 300, mounted by von Ardenne Anlagentechnik, Dresden, Germany). The rotatable dual magnetron (RDM) cathodes with ZnO ceramic tube targets, which are 760 mm in length and 160 mm in diameter and doped with 0.5 wt% Al_2O_3, were operated at a discharge power of 14 kW in total with a mid-frequency (MF) of 40 kHz. 200 sccm pure argon was introduced as sputtering gas during sputtering. The substrate temperature and working pressure were 350°C and 2 Pa, respectively. The magnetron mounting allows the magnetrons to tilt directions in steps of 30° as shown in **Fig. 1**. In case A, both magnetrons are in standard orientations and their main directions are perpendicular to the substrate as shown in **Fig. 1** (A). In other cases, both magnetrons are tilted by 30° towards the center of the double cathodes (B) and towards the outside region (C). **Fig. 1** presents the cathode-substrate system with tube targets, substrate, inside tilted magnetrons and the racetracks on the cathodes, as well as slash zones on the substrates, which indicate the pounding by high energetic particles coming from racetracks of the cathodes. A few special positions are marked with letters (a-i) on substrates in three cases as shown in **Fig. 1**. More details about the configuration of this system can be found in reference [**18, 19, 20**]. The rotating speed for both ceramic targets is 10 rpm. Before the deposition pre-sputtering for about 10 minutes was carried out. The substrate holder is moved within 7 seconds from the pre-sputtering position to the position for static deposition. The deposition times for case A, B and C are 3 minutes, 3 minutes

and 7 minutes, respectively. The thickness of the deposited film was measured utilizing surface profiler (Dektak 3030, Veeco Instruments Inc). The electrical properties of the films deposited at various positions were investigated by Hall effect measurement using van der Pauw method (Keithley 926 Hall set-up). The morphologies of ZnO:Al films after a chemical etching step in diluted hydrochloric acid (HCl) by an in-line etching system were evaluated by atomic force microscopy (AFM) (Surface Imaging System (SIS), Nano Station 300).

3. Results

3.1. Deposition rate

Fig. 2 shows the variation of deposition rate of ZnO:Al films, which were statically deposited with differently tilted magnetrons (cases A, B and C), as a function of substrate position along lateral direction (x-axis). In case A (open square), two local maxima of the static deposition rate (~350 nm/min) occur at x-positions -7 cm and 10 cm corresponding to the target positions (see also positions (a) and (c) in **Fig. 1**). A minimal static deposition rate of around 260 nm/min appears in the center of the cathodes (around substrate position b) and the deposition rate decreases towards other regions. In case B (open circle), one approximately 10 cm wide flat plateau of maximum 460 nm/min is found in the center of the substrate. Towards the edges of the substrate, the local static deposition rate drops to approximate 160 nm/min. Case C (open triangle) shows the similar deposition rate profile on case A and a much more pronounced minimum static deposition rate of 90 nm/min in the center (at substrate position h in **Fig. 1**). The highest static deposition rate near the margin of substrate is 270 nm/min, which is a factor of three higher than that of center position.

The dynamic deposition rates here, which are the integration results of static deposition rates during the length across the plasma space (0.3 m here), are also shown in **Fig. 2** (horizontal lines). In fact, the dynamic deposition rate indicates that how thick a film would be when the carrier moves with a moving speed of 1 m/min in on-line industrial production. In case A, the dynamic deposition rate is about 99 nm·m/min. In case B, the dynamic deposition rate is about 111 nm·m/min while it is only about 59 nm·m/min in case C. The experimental dynamic deposition rates for each case (solid symbols) are given as well. They seem a little lower than calculated values. It could be due to that relatively low deposition rates at border. Moreover, the slight change of plasma during dynamic sputtering deposition could have a small role in dynamic deposition rate to some extent.

3.2. Electrical properties

Figs. 3-5 show the thickness (t), resistivity (ρ), carrier concentration (n) and Hall mobility (μ) of ZnO:Al films statically deposited in case A, B and C, and are plotted as a function of position along lateral direction. The slash areas correspond to substrate regions affected by the racetracks as shown in **Fig. 1**. These slash areas show high resistivities and low carrier concentrations. In case C and at the outer racetracks of case A both films also show minima in mobility. However, the lowest mobility is found in the center of case C. The lowest resistivity is always found next to racetrack positions and even more pronounced between the two racetracks of each target. This is due to the increase in carrier concentration (n) and Hall mobility (μ) as shown in **Figs. 3-5** (**b** and **c**). Low deposition rates lead to a low conductivity, even if the thickness is above 700 nm. The lowest resistivity down to 3.2×10^{-4} Ω·cm at substrate position 2 cm of thin film in case B was achieved. The lowest resistivities in case A symmetrically appear at substrate positions -8 cm and 10 cm (about positions (a) and (c)). The lowest resistivities in case C also symmetrically appear at substrate positions near the slash regions (about positions (g) and (i)). The general observations on resistivity with respect to the racetrack positions are similar to other researchers reported on ZnO:Al films [**11, 12, 13**].

3.3. Etching behavior and morphology

The ZnO:Al film deposited under condition A was etched by an in-line etching system. Due to the uniform etching of the process itself, all variations of etching behavior are caused by different ZnO:Al material properties. **Fig. 6** shows the position-dependent thickness before (open circles) and after etching (open triangles) as well as the removed thickness (solid squares) of the ZnO:Al films. Around substrate positions (a) and (c) (at the center of each target) the films show the lowest removed film thicknesses. The ZnO:Al films, located at the enter of the cathode system (between -2 cm and 3 cm, at about substrate position b), exhibit a minimum in thicknesses before and after etching. The etch rate at these regions is about a factor of 5 higher than that in the regions in front of the targets. Etch rate at the left margin areas on the film increases towards outer regions as the initial thickness decreases. This behavior is not visible at the right, since the right outer regions have not been covered by the substrate.

The topography of the ZnO:Al film after etching is known to be very sensitive to ZnO:Al material properties [**2, 9**] and therefore it is used to identify position-dependent characteristics of ZnO:Al films. AFM measurements were carried out at several positions. As characteristic examples the AFM images taken at positions 2 cm, 4 cm and 13 cm are shown in **Fig. 7(a-c)**, respectively. The AFM image at position 2 cm corresponding to the highest etch rate shows shallow features of about

500 nm lateral size covered with additional small hillocks and represents the etched morphologies at three measured substrate positions between 0 cm and 3 cm. **Fig. 7(b)** shows the surface structure of the thin film after etching at position 4 cm with moderate etch rate. It represents the same surface structure of film at symmetric position -2 cm. Distinct and deep carters regularly distribute on the surface of the ZnO:Al film. **Fig. 7(c)** displays the surface structure of the etched film at position 12 cm, which exhibits the lowest etch rate. Positions from -10 cm to -3 cm as well as from 6 cm to 15 cm on this etch film with low etch rates and exhibit similar surface structures with only a few craters of more than 1 μm diameter in more or less flat areas. Moreover, a dynamically deposited ZnO:Al film was prepared under condition A in order to compare with this ZnO:Al film prepared in static mode. The surface texture after etching is shown in **Fig.7 (d)**. The dynamically deposited ZnO:Al film develops a similar surface structure after etching, which is similar to etched ZnO:Al films sited opposite to each target in static mode (case A).

4. Discussion

The cathode-substrate configurations with different magnetron tilt angles lead to different deposition rate profiles. The results can be understood if one considers each racetrack on the tube surface as an independent sputter source of ZnO:Al films with radial beam of sputtered particles as indicated in **Fig. 1**. However, the static prints cannot resolve each racetrack in thickness profiles. Thereby only two peaks are visible for each target in case A. Both peaks even can merge to one peak in case B due to an overlap of the deposition zones of both targets. Substrate area is limited and meanwhile metal sheets shield sputtered material towards outer regions of substrates during dynamic deposition. As a consequence, the dynamic deposition rate will strongly reduce if magnetrons are tilted outwards for case C.

The higher resistivity as well as lower carrier concentration and Hall mobility at racetrack positions are mainly attributed to highly energetic oxygen ion bombardment [**11, 21, 13**]. The highly energetic particles can induce internal stresses and local defects [**23, 24**]. Moreover, the strong impact of oxygen may form aluminum oxide or excess oxygen inside ZnO:Al films. Both effects reduce doping efficiency and then the carrier density. In film areas with low deposition rate the mobility as well as carrier density drop due to a lower film thickness, which is especially relevant for doping concentrations below 1 wt% [**25**]. Best electrical properties of ZnO:Al films appear at regions with high deposition rate as well as with low impact of the ion bombardment next to the racetracks.

Upon a chemical wet etching step in diluted HCl the ZnO:Al films develop different surface structures. Three different topographies were observed and identified as type A, B and C as classified by Kluth et al. [**2**]. According to the observations by Hüpkes et al. [**11**], the substrate positions faced to racetracks show lower etching rates as in our case. However, the etch rates between the racetracks of each target also exhibit low etch rates and indicate to highly compact films in these regions[**2**]. A relatively high working pressure of 2 Pa was used here that might spread the effect of ion bombardment to a wider substrate area due to high diffusion of sputtered particles [**26**]. Another reason could be the strong heat impact by the high rate sputter process directly in front of the targets. Similar to the observations by Hüpkes in the center of cathode system ZnO:Al shows a high etching rate. The longer path of the sputtered particles from the target to the substrate leads to about 50 % more collisions with other gas atoms. This provides similar effects like higher gas pressure that leads to such results [**2**].

The dynamic deposition forms a multilayer system of the material observed in the static case. The dynamic deposition rate can be calculated from the profile of static deposition rate. The electrical properties are a superposition of the lateral variations of the electrical properties and even the etching behavior is dominated by conditions that are widely present in static mode. The low etch rate and surface topographies with only few craters on dynamically deposited ZnO:Al films are widely presented in static mode.

5. Conclusions

ZnO:Al films were prepared at a high discharge power from rotatable dual tube targets with tilted magnetrons inside. The experimental results reveal the decisive influence of the magnetron configurations on electrical and structural properties of ZnO:Al films at different positions. The highest static and dynamic deposition rates of up to 360 nm/min and 111 nm·m/min, respectively, were obtained by tilting the magnetrons inwards to the center of the substrate. ZnO:Al films grown in radial direction in front of the racetracks exhibit higher resistivity, lower carrier concentrations and lower Hall mobility caused by highly energetic oxygen ion bombardment whereas high mobility is mainly governed by film thickness. In front of the targets between racetracks best electrical properties were obtained with mobility of nearly 50 cm^2/Vs. The ZnO:Al films before and after etching at different substrate positions for standard magnetron configuration show different surface structures and were classified in three different material types. The dynamically deposited ZnO:Al film seems to be dominated by material properties, which dominate the properties of statically deposited films. This indicates that an optimization of dynamically sputtered

ZnO:Al films requires an examination of the static print on each position. This is a challenge for the design of optimized surface-textured ZnO:Al films for silicon thin film solar cells. Tilted magnetrons might be an additional option to tune the material properties in dynamic deposition.

Acknowledgement

The authors would like to thank J. Owen and W. Zhang for great help in AFM measurements of these samples. This study was financially supported by German ministry BMU under contract number 0327693A and Shanghai Municipal Science & Technology Committee under contract number 09JC1404600.

Reference

[1] B. Rech, H. Wagner, Appl. Phys. A 69 (1999) 155.
[2] O. Kluth, G.. Schöpe, J. Hüpkes, C. Agashe, J. Müller, B. Rech, Thin Solid Films 442 (2003) 80.
[3] M. Berginski, J. Hüpkes, M. Schlute, G.. Schöpe, H. Stiebig, M. Wuttig, J. Appl. Phys. 101 (2007) 074903-1.
[4] J. Müller, G. Schöpe, O. Kluth, B. Rech, M. Ruske, J. Trube, B. Szyszka, X. Jiang and G. Brauer, Thin Solid Films 392 (2001) 327.
[5] B. Szyszyka. Thin Solid Films 351 (1999) 164.
[6] T. Tohsophon, J. Hüpkes, H. Siekmann, B. Rech, M. Schulteis and N. Sirikulrat, Thin Solid Films 516 (2008) 4628.
[7] V. Sittinger, W. Dewald, W. Werner, B. Szyszka, F. Ruske, Photovoltaics International, Sixth Edition, November 2009, p. 101-108.
[8] H. Sato, T. Minami and S. Takata, T. Mouri and N. Ogawa, Thin solid Films 220(1992)327.
[9] J. Hüpkes, B. Rech, O. Kluth, T. Repmann, B. Zwaygardt, J. Müller, R. Drese, M. Wuttig, Sol. Energy. Mater. Sol. Cells 90 (2006) 3054.
[10] J. F. Chang, M. H. Hon, Thin Solid Films. 386 (2001) 79.
[11] J. Hüpkes, B. Rech, O. Kluth, J. Müller, H. Siekmann, C. Agashe, H. P. Bochem and M. Wuttig, Proceeding in MRS Spring Metting, 2003, Volume 762, A7.11.
[12] T. Minami, J. Vac.Sci. Technol. A 18 (2000) 1584.
[13] T. Minami, H. Nanto, H. Sato, S. Takata, Thin Solid Films 164 (1988) 275.
[14] F. Fenske, W. Fuhs, E. Nebauer, A. Schöpke, B. Selle, I. Sieber, Thin Solid Films 343-344 (1999) 130.

[15] H. Zhu, E. Bunte, J. Hüpkes, H. Siekmann, S. M. Huang, Thin Solid Films 517 (2008) 3161.

[16] J. Müller, J. Liu, J. Schroeder, D. Marquardt and R. Trassl, 22nd European Photovoltaic Solar Energy Conference, Milan, Italy, 2007, p. 2229.

[17] E. Bunte, H. B. Zhu, J. Hüpkes, Proceeding of 23rd European Photovoltaic Solar Energy Conference, 1-5 September 2008, Valencia, Spain, p2105.

[18] J. Hüpkes, H. Zhu, J. I. Owen, G. Jost, E. Bunte, Proceedings of the 8th International Conference on Coatings on Glass and plastics, 2010, Braunschweig, Germany, p439.

[19] E. Bunte, J. Hüpkes, H. Zhu, M. Berginski, H. Siekmann, W. Appenzeller, B. Rech, Proceeding of 22nd European Photovoltaic Solar Energy Conference, 3-7 September 2007, Milan, Italy, p2173.

[20] H. Zhu, J. Hüpkes, E. Bunte, S. M. Huang, Appl. Surf. Sci, 256 (2010)4601.

[21] K. Tominaga, K. Kuroda and O. Tada, Jpn. J. Appl. Phys 27 (1988) 1176.

[22] T. Minami, H. Nanto, H. Sato and S. Takata, Thin Solid Films 164 (1988) 275.

[23] I. Petrov, V. Orlinov, A. Misiuk, Thin Solid Films 120 (1984) 55.

[24] J. Hinze and K. Ellmer, J. Appl. Phys 88 (2000) 2443.

[25] C. Agashe, O. Kluth, J. Hüpkes, U. Zastrow and B. Rech, J. Appl. Phys.95 (2004) 1911.

[26] T. P. Drüsedau, M. Löhmann, B. Garke, J. Vac. Sci. Technol. A 16 (1998) 2728.

Captions

Fig. 1. Schematic diagram of cathode-substrate system with different magnetron orientations: case A, both magnetrons are parallel and their main direction is vertical to the substrate; case B. both magnetron angles deviate from the normal direction of substrate by 30° and are towards the inner sides of targets one another; case C, magnetron angles deviate from the normal direction of substrate by 30° as well but towards outer sides of targets.

Fig. 2. Static and calculated dynamic deposition rates in three cases (open square for case A, open circle for case B and open triangle for case C) and corresponding experimental dynamic deposition rates as a function of substrate position along lateral direction (x-axis direction).

Fig. 3. Thickness and electrical properties (resistivity(ρ), carrier concentration(n) and Hall mobility(μ)) of the film deposited in case A, as a function of substrate position.

Fig. 4. Thickness and electrical properties (resistivity(ρ), carrier concentration(n) and Hall mobility(μ)) of the film deposited in case B, as a function of substrate position.

Fig. 5. Thickness and electrical properties (resistivity(ρ), carrier concentration(n) and Hall mobility(μ)) of the film deposited in case C, as a function of substrate position.

Fig. 6. The thickness of the ZnO:Al films deposited in case A before and after etching in a dilute HCl (0.5%) by an in-line etching system, as well as the removed thickness as a function of substrate position.

Fig. 7. The AFM images of the etched ZnO:Al films static deposited in case A at x-positions 2 cm, 4 cm and 12 cm as well as the AFM image of the ZnO:Al film deposited in dynamic mode under condition A.

Zhu_ Fig. 1.tif

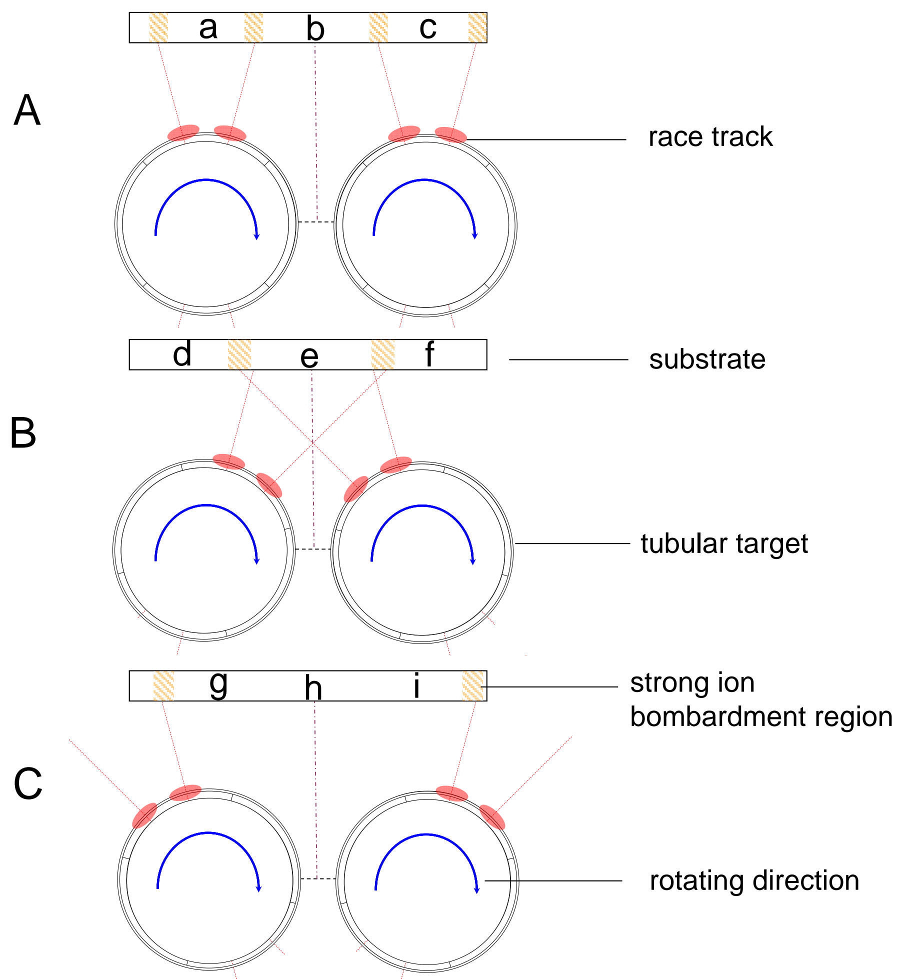

Zhu_ Fig. 2.tif

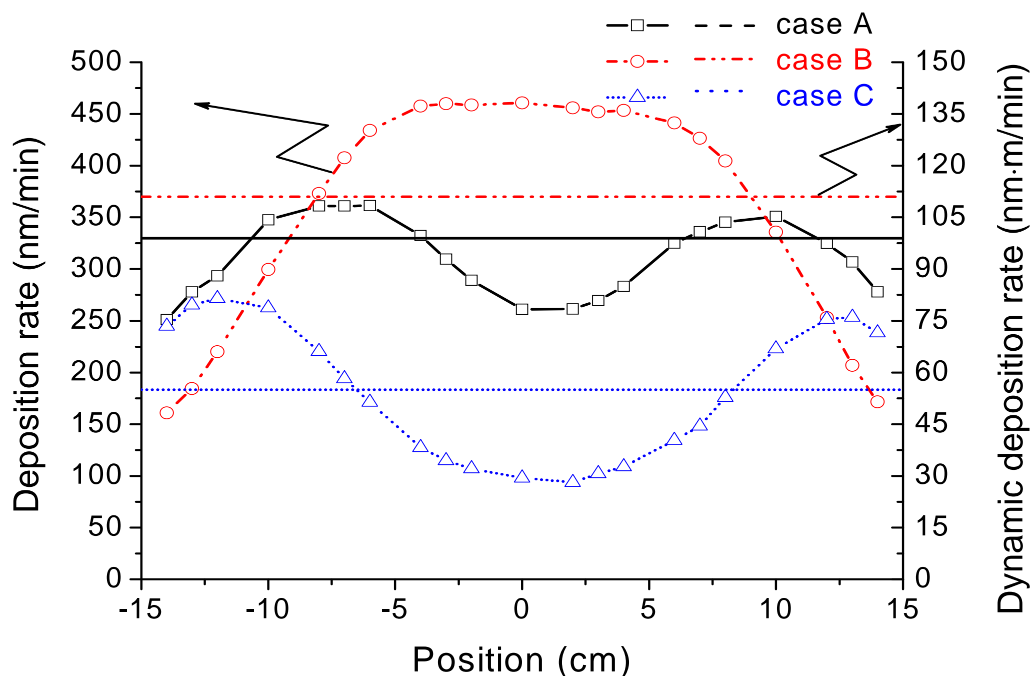

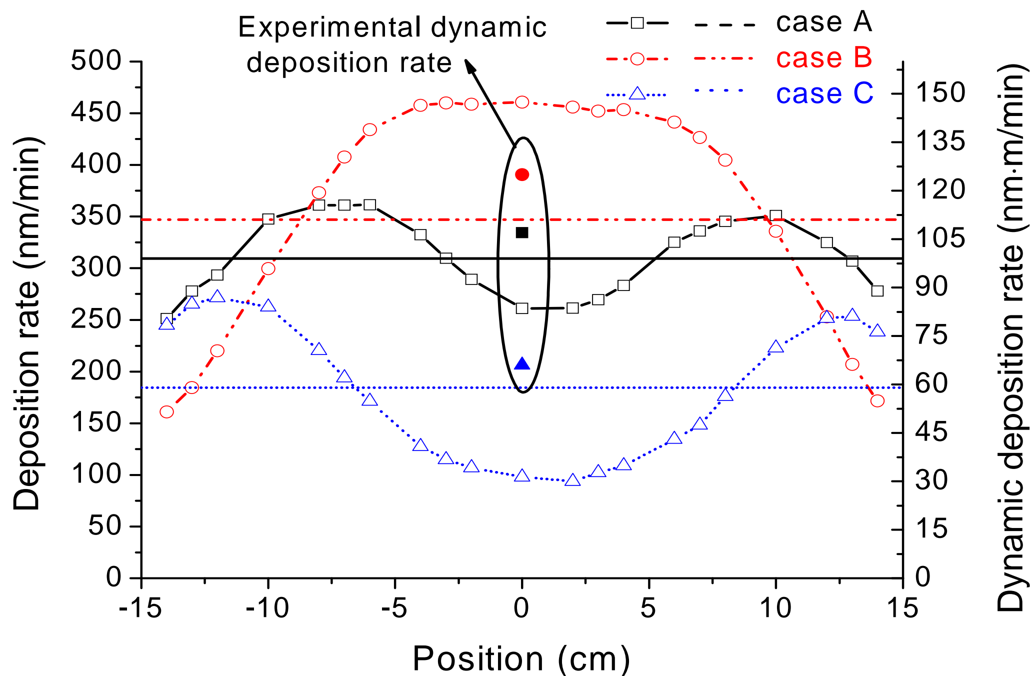

Zhu_ Fig. 3.tif

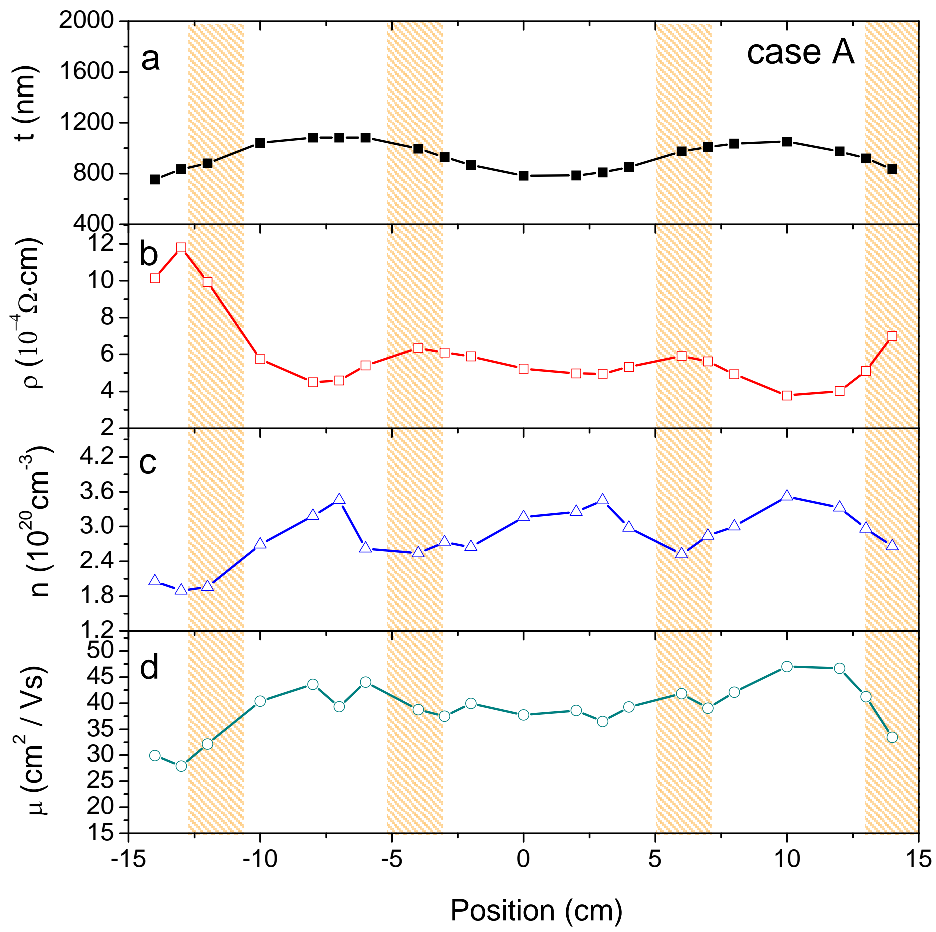

Zhu_ Fig. 4.tif

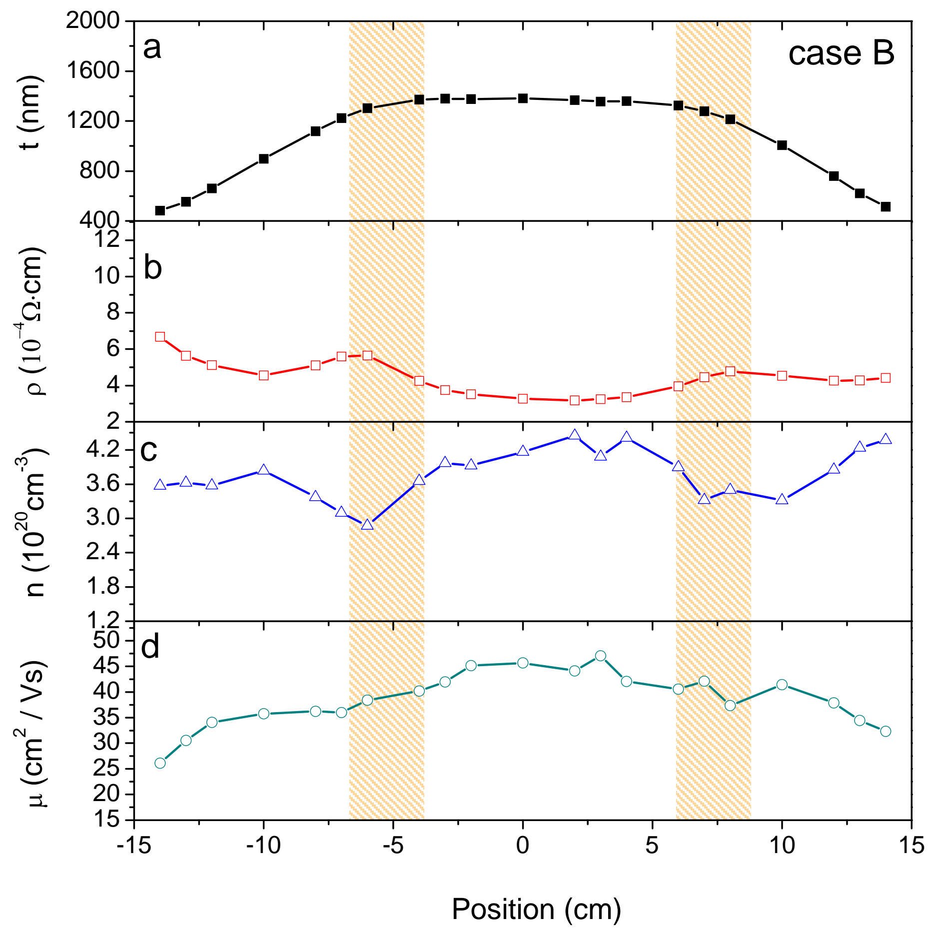

Zhu_ Fig. 5.tif

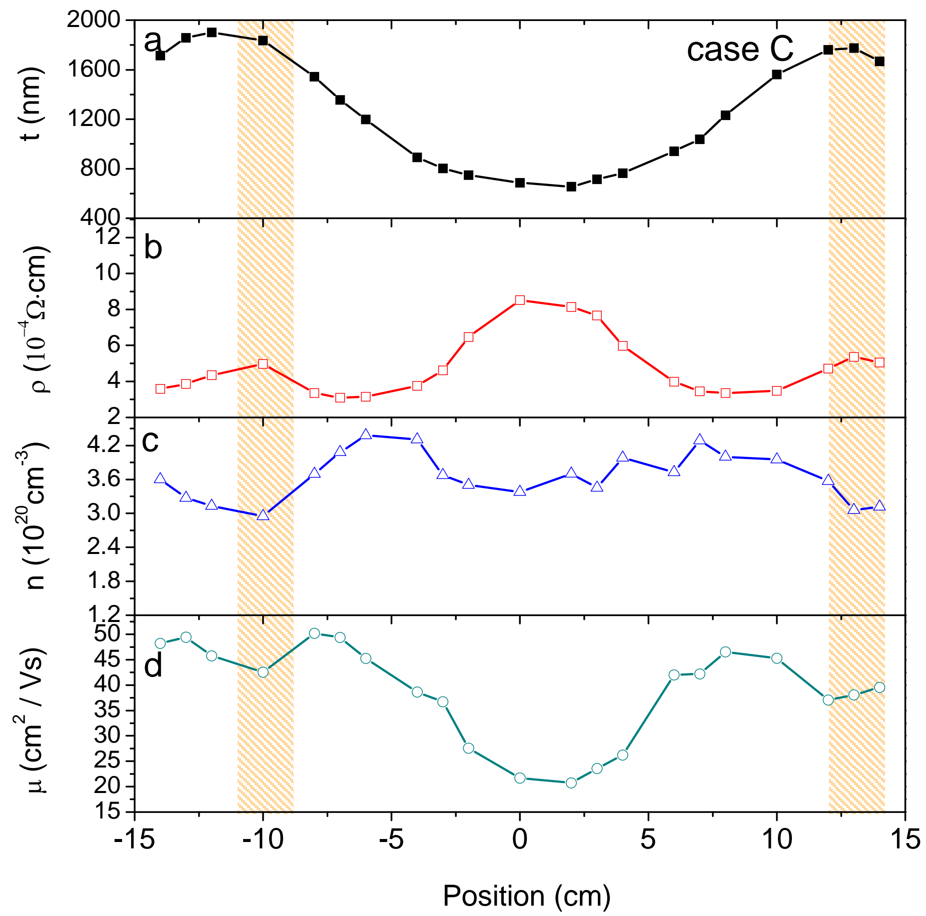

Zhu_ Fig. 6.tif

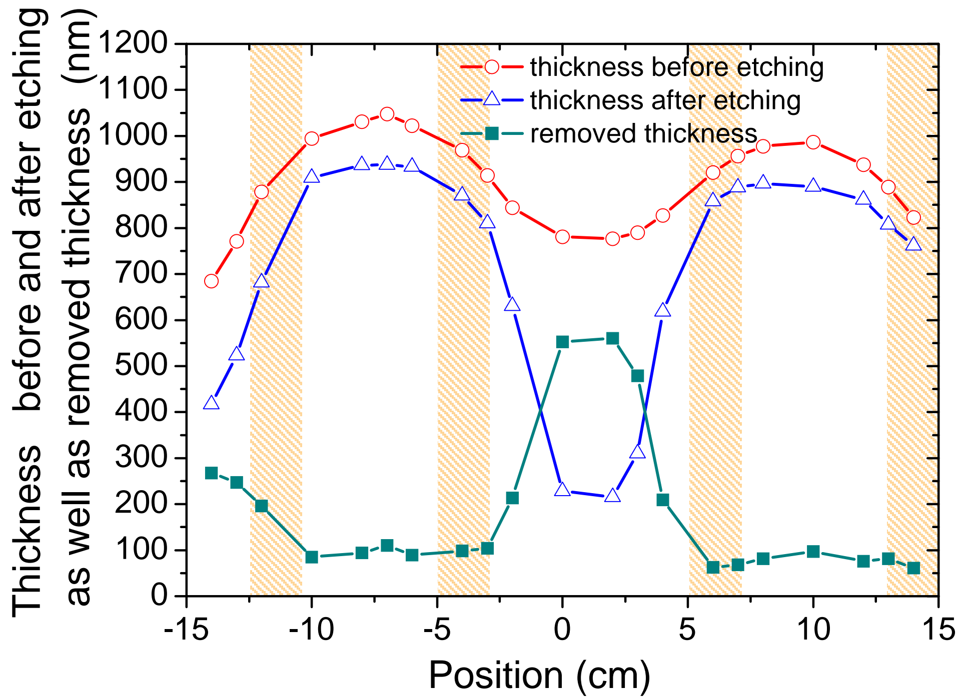

Zhu_ Fig. 7

a)

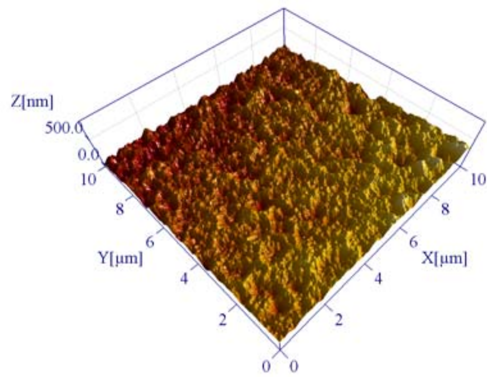

b)

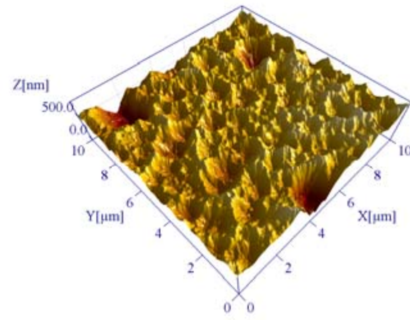

c)

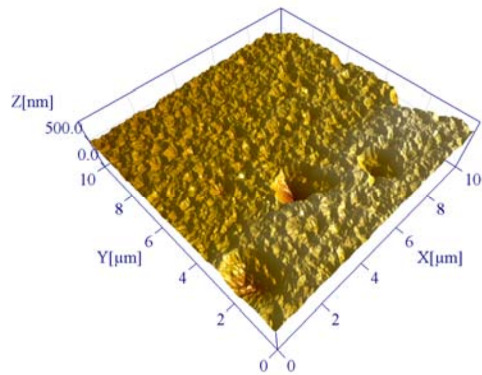

d)